Inorg. Chem. 1990, 29, 2487-2495

Contribution from the Department of Chemistry, University of Western Ontario, London, Ontario, Canada N6A 5B7,
and Chemistry Division, National Research Council of Canada,[†] Ottawa, Ontario, Canada K1A 0R9

Electronic Structure of *cis*-Dimethylplatinum(II) Complexes from UV Photoelectron Spectra and SCF–MS–Xα Calculations

Dong-Sheng Yang,[‡] G. Michael Bancroft,[*,‡] Lisa Dignard-Bailey,[‡] Richard J. Puddephatt,[*,‡] and John S. Tse[§]

Received May 5, 1989

UV photoelectron spectra of *cis*-$[PtMe_2L_2]$ [L = PMe_3, PMe_2Ph, $PMePh_2$, PEt_3, $P(NMe_2)_3$, $PMe(OEt)_2$, $P(OMe)_3$, $P(OEt)_3$, $AsMe_3$, CNMe, CNPh; L_2 = $Me_2NCH_2CH_2NMe_2$ (TMED), 1,5-cyclooctadiene (COD), norbornadiene (NBD)] are reported, as well as MS–Xα calculations on the model compounds *cis*-$[PtMe_2(EH_3)_2]$ (E = N, P, As), *cis*-$[PtMe_2(C_2H_4)_2]$, and *cis*-$[PtMe_2(CNH)_2]$. The results from these calculations and spectral information, such as resolved vibrational fine structures and ligand shift effects, have allowed the assignment of the lower energy ionizations to specific molecular orbitals. The two molecular orbitals with lowest ionization energies are assigned, in all cases, to Pt–ligand σ orbitals, and these are followed by four MO's that have mostly nonbonding Pt 5d character. The σ-donor ability of a ligand L is reflected in the first ionization energy and decreases in the order L = $P(NMe_2)_3$ > TMED > $PMePh_2$ ~ PMe_2Ph > PEt_3 > $AsMe_3$ ~ PMe_3 > $PMe(OEt)_2$ > $P(OEt)_3$ > $P(OMe)_3$ > COD > NBD. The π-acceptor ability is reflected by the energy separation of the Pt d_{xy} and d_{xz} (axes defined by C_{2v} symmetry) and falls in the order $PMePh_2$ ~ PMe_2Ph ~ $P(OMe)_3$ ~ $P(OEt)_3$ ~ $PMe(OEt)_2$ ~ $P(NMe_2)_3$ > $AsMe_3$ ~ PMe_3 ~ PEt_3 ~ COD ~ NBD > TMED. Both isocyanide ligands CNMe and CNPh, which cannot be arranged into the above series, have comparable σ-donor ability, and the latter has stronger π-donor and π-acceptor properties. Some typical chemical processes are also discussed on the basis of the established σ/π series.

Introduction

The complexes *cis*-$[PtR_2L_2]$, where R = alkyl or aryl and L = a ligand such as a tertiary phosphine or arsine, amine, alkene, or isocyanide, have played an important role in studies of organometallic reaction mechanisms related to catalysts by d^8 complexes, and the more volatile compounds are useful precursors for chemical vapor deposition of platinum.[1-7] However, there has not been any experimental determination of the relative energies of the valence orbitals, in particular the σ-PtC and Pt 5d orbitals in these molecules. Preliminary studies using photoelectron spectroscopy of some of these complexes have been reported, but since only He I spectra and no complementary theoretical calculations were available, only tentative assignments were given.[8] Since a knowledge of bonding, in particular the orbital energies of high occupied orbitals, is important in understanding reactivity and mechanism,[1-7,9] we have undertaken a detailed He I and He II photoelectron spectroscopic study of complexes *cis*-$[PtMe_2L_2]$, where L = PMe_3, PMe_2Ph, $PMePh_2$, PEt_3, $P(NMe_2)_3$, $PMe(OEt)_2$, $P(OMe)_3$, $P(OEt)_3$, AsMe, CNMe, and CNPh or L_2 = $Me_2NCH_2CH_2NMe_2$ (TMED), 1,5-cyclooctadiene (COD), and norbornadiene (NBD). To aid in assignments and to predict the nature of low unoccupied molecular orbitals, we have also carried out SCF–MS–Xα calculations on the model compounds *cis*-$[PtMe_2(EH_3)_2]$ (E = N, P, As), *cis*-$[PtMe_2(C_2H_4)_2]$, and *cis*-$[PtMe_2(CNH)_2]$. A preliminary communication on the alkene complexes only has been published recently.[10]

Experimental Section

All compounds were synthesized by the same method, and a typical example is given. To a suspension of $[Me_4Pt_2(\mu\text{-}SMe_2)_2]$[11] (0.200 g, 0.348 mmol) in dry CH_2Cl_2 (5 mL) in a Schlenk tube was added triethylphosphine (0.21 mL, 1.40 mmol) under N_2 at room temperature. After 40 min, the solvent was removed under vacuum to yield a white residue of *cis*-$[PtMe_2(PEt_3)_2]$, which was purified by sublimation at 85 °C and 10^{-2} mmHg to yield a white solid (0.20 g, 62.4% yield). The purity and identity of known complexes were checked by their melting points and NMR spectra. The new compounds were also confirmed by elemental analysis and/or mass spectrometry. $[PtMe_2\{P(NMe_2)_3\}_2]$: white solid, mp 97 °C. ^{1}H NMR ($CDCl_3$): δ 0.38 [^2J(Pt–H) = 66.0 Hz, Pt–CH_3], 2.65 (s, NMe). ^{31}P NMR ($CDCl_3$): δ 116.22 [J(Pt–P) = 2841.0 Hz, Pt–$P(NMe_2)_3$]. Molecular weight: 551 (mass spectrum). Anal. Calcd for $C_{14}H_{42}N_6P_2Pt$: C, 30.46; H, 7.68; N, 15.25. Found: C, 30.19; H, 7.89; N, 15.59. *cis*-$[PtMe_2(P(OEt)_3)_2]$: yellow liquid. ^{1}H NMR ($CDCl_3$): δ 0.53 [^2J(Pt–H) = 67.0, Pt–CH_3], 1.29 (t, OCH_2CH_3), 4.02 (q, OCH_2). ^{31}P NMR ($CDCl_3$): δ 130.65 [J(Pt–P) = 3106.1 Hz, Pt–$P(OEt)_3$]. Molecular weight: 557 (mass spectrum). *cis*-$[PtMe_2(PMe(OEt)_2)_2]$: green-yellow liquid. ^{1}H NMR ($CDCl_3$): δ 0.43 [^2J(Pt–H) = 65.3 Hz, Pt–CH_3], 1.56 (d, PMe), 1.25 [t, OCH_2CH_3], 3.93 (q, OCH_2). ^{31}P NMR ($CDCl_3$): δ 152.5 [J(Pt–P) = 2591.0 Hz, Pt–$PMe(OEt)_2$]. Molecular weight: 497 (mass spectrum).

The photoelectron spectra were recorded on a McPherson ESCA-36 photoelectron spectrometer equipped with a hollow-cathode UV He lamp,[12] at temperatures within 30 °C of the melting point of each complex. The argon $^2P_{3/2}$ ionization at 15.76 eV was used as internal calibration during data acquisition. The resolutions (fwhm of Ar $^2P_{3/2}$ ionization) were less than 0.027 and 0.036 eV for the He I and He II sources, respectively. Spectra were fitted to Lorentzian–Gaussian line shapes with the use of an iterative procedure,[13] with reproducibility of the vertical ionization energy (IE) of ±0.02 eV in most cases. In the most poorly resolved spectra the reproducibility was ±0.05 eV. The relative band areas are reproducible to about 10% in the He I spectra and about 15% in the He II spectra. The band area ratios from He I and He II

[†] NRCC Contribution No. 29890.

[‡] University of Western Ontario.

[§] National Research Council of Canada.

(1) Braterman, P. S.; Cross, P. J.; Young, G. B. *J. Chem. Soc., Dalton Trans.* **1976**, 1306, 1310.

(2) Balazs, A. C.; Johnson, K. H.; Whitesides, G. M. *Inorg. Chem.* **1982**, *21*, 2162.

(3) Obara, S.; Kitaura, K.; Morokuma, K. *J. Am. Chem. Soc.* **1984**, *106*, 7482.

(4) Low, J. H.; Goddard, W. A., III *Organometallics* **1986**, *5*, 609.

(5) Appleton, T. G.; Berry, R. D.; Hall, J. R.; Neale, D. W. *J. Organomet. Chem.* **1988**, *342*, 399.

(6) Miller, T. M.; Izumi, A. N.; Shih, Y. S.; Whitesides, G. M. *J. Am. Chem. Soc.* **1988**, *110*, 3146. Miller, T. M.; McCarthy, T. J.; Whitesides, G. M. *J. Am. Chem. Soc.* **1988**, *110*, 3156. Miller, T. M.; Whitesides, G. M. *J. Am. Chem. Soc.* **1988**, *110*, 3164.

(7) Kumar, R.; Roy, S.; Rashidi, M.; Puddephatt, R. J. *Polyhedron* **1989**, *8*, 551.

(8) Behan, J.; Johnstone, R. A. W.; Puddephatt, R. J. *J. Chem. Soc., Chem. Commun.* **1978**, 444.

(9) Louwen, J. N.; Hengelmolen, R.; Grove, D. M.; Oskam, A. *Organometallics* **1984**, *3*, 908. Louwen, J. N.; Grove, D. M.; Ubbels, H. J. C.; Stufkens, D. J.; Oskam, A. *Z. Naturforsch., B* **1983**, *38*, 1657. Oskam, A.; Stufkens, D. J.; Louwen, J. N. *J. Mol. Struct.* **1986**, *142*, 347. Bella, S. D.; Fragalia, I.; Granozzi, G. *Inorg. Chem.* **1986**, *25*, 3997. Granozzi, G.; Zangrande, G.; Bonivento, M.; Michelon, G. *Inorg. Chim. Acta* **1983**, *77*, L229. Zangrande, G.; Granozzi, G.; Casarin, M.; Daudey, J. P. *Inorg. Chem.* **1986**, *25*, 2872. Louwen, J. N.; Hengelmolen, R.; Grove, D. M.; Stufkens, D. J.; Oskam, A. *J. Chem. Soc., Dalton Trans.* **1986**, 141. Granozzi, G.; Vittadini, A.; Sindellari, L.; Ajo, D. *Inorg. Chem.* **1984**, *23*, 702.

(10) Yang, D. S.; Bancroft, G. M.; Bozek, J. D.; Puddephatt, R. J.; Tse, J. S. *Inorg. Chem.* **1989**, *28*, 1.

(11) Scott, J. D.; Puddephatt, R. J. *Organometallics* **1983**, *2*, 1643.

(12) Coatsworth, L. L.; Bancroft, G. M.; Creber, D. K.; Lazier, R. J. D.; Jacobs, P. W. M. *J. Electron Spectrosc. Relat. Phenom.* **1978**, *13*, 395.

(13) Bancroft, G. M.; Adams, J.; Coatsworth, L. L.; Bennewitz, C. D.; Brown, J. D.; Westwood, W. D. *Anal. Chem.* **1975**, *47*, 586.

0020-1669/90/1329-2487\$02.50/0

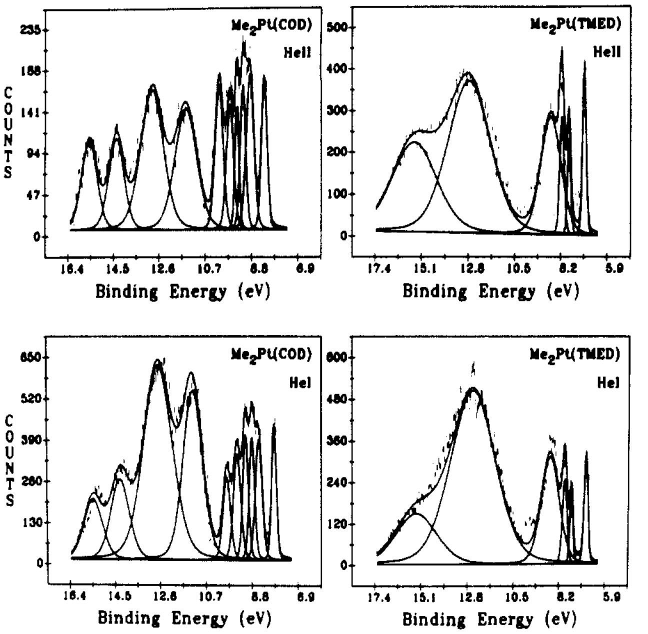

Figure 1. He I and He II spectra of *cis*-[PtMe$_2$L$_2$] (L$_2$ = COD and TMED).

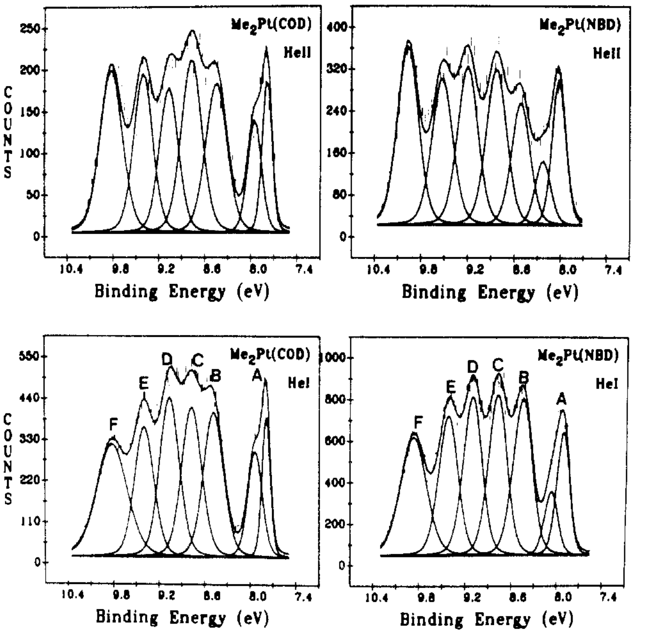

Figure 2. He I and He II spectra in the low ionization energy region of *cis*-[PtMe$_2$L$_2$], where L$_2$ = COD and NBD.

spectra were corrected for the electron analyzer transmission energy, by dividing by the kinetic energy of the band.

The calculations presented here were performed by using the relativistic version of the Xα scattered-wave method,[14] in which the relativistic radial wave functions of the Pt atom have been employed. For comparison, a nonrelativatistic calculation was also performed on the ground state of *cis*-[PtMe$_2$(PH$_3$)$_2$]. The exchange α parameters used in each atomic region were taken from Schwarz's tabulation,[15] except for hydrogen, for which 0.777 25 was used.[16] For the extramolecular and intersphere regions, a weighted average of the atomic α's was employed, the weights being the number of valence electrons in neutral atoms.[17]

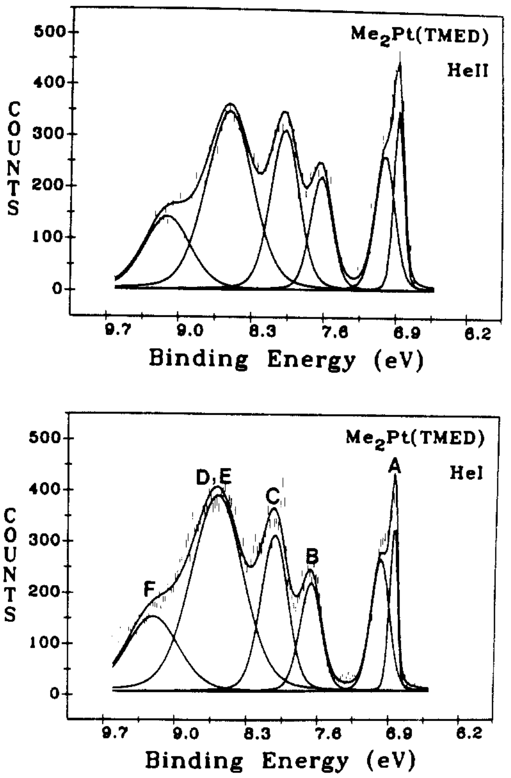

Figure 3. He I and He II spectra of *cis*-[PtMe$_2$(TMED)].

Table I. Ionization Energies (eV) and Assignments of Bands for *cis*-[PtMe$_2$L$_2$]

band	orbital	COD	NBD	TMED	AsMe$_3$
A	4a$_1$	7.76, 7.93	7.91, 8.06	6.85, 6.98	7.30
B	2b$_2$	8.47	8.45	7.67	7.60
C	3a$_1$	8.76	8.77	8.03	7.91
D	1b$_1$	9.05	9.10	8.59	8.28
E	1a$_2$	9.39	9.42		8.67
F	2a$_1$	9.82	9.87	9.20	8.98

band	orbital	MeNC	PhNC
A	5a$_1$	7.60	
B	4a$_1$	7.98	8.16
C	3b$_2$	8.31	
D	2b$_1$	8.70	
E	2a$_2$	9.12	9.04
F	3a$_1$	9.59	9.26
	Ph (π)		9.91, 10.57

Overlapping sphere radii were used.[18,19] An l_{max} of 3 was used around the outer-sphere region and the Pt atom, whereas an l_{max} of 2, 1, and 0 was used around As and P, N, and H atoms, respectively. The geometries were based on the X-ray data of similar compounds and were assumed to have C_{2v} symmetry.[20]

---

(14) Johnson, K. H. *Adv. Quantum Chem.* **1973**, *7*, 147. Herman, F.; Williams, A. R.; Johnson, K. H. *J. Chem. Phys.* **1974**, *61*, 3508. Case, D. A.; Yang, C. Y. *Int. J. Quantum Chem.* **1980**, *18*, 1091. Cook, M.; Case, D. A. *QCPE* **1982**, *14*, 465.

(15) Schwarz, K. *Phys. Rev. B* **1972**, *5*, 2466; *Theor. Chim. Acta* **1974**, *34*, 225.

(16) Slater, J. C. *Int. J. Quantum Chem.* **1973**, *7S*, 533.

(17) Exchange factors for extramolecular and intersphere regions: Me$_2$Pt(NH$_3$)$_2$, 0.74629; Me$_2$Pt(PH$_3$)$_2$, 0.73985; Me$_2$Pt(AsH$_3$)$_2$, 0.73496; Me$_2$Pt(C$_2$H$_4$)$_2$, 0.75073; Me$_2$Pt(CNH)$_2$, 0.74583; Me$_2$Pt, 0.73618; NH$_3$, 0.71645; PH$_3$, 0.74534; AsH$_3$, 0.73313; C$_2$H$_4$, 0.76527; CNH, 0.75742.

(18) Norman, J. G., Jr. *J. Chem. Phys.* **1974**, *61*, 4630; *Mol. Phys.* **1976**, *31*, 1191.

(19) Atomic and outer-sphere radii (bohrs) are as follows. Me$_2$Pt(NH$_3$)$_2$: outer, 6.1052; Pt, 2.6512; C, 1.6476; N, 1.5651; H$_C$, 1.1880; H$_N$, 1.1605. Me$_2$Pt(PH$_3$)$_2$: outer, 6.3916; Pt, 2.6512; C, 1.6794; P, 2.2564; H$_C$, 1.1880; H$_P$, 1.3410. Me$_2$Pt(AsH$_3$)$_2$: outer, 6.7935; Pt, 2.6577; C, 1.6794; As, 2.3907; H$_C$, 1.2010; H$_{As}$, 1.3890. Me$_2$Pt(C$_2$H$_4$)$_2$: outer, 6.8965; Pt, 2.6577; C, 1.6794; H, 1.2390. Me$_2$Pt(CNH)$_2$: outer, 7.4599; Pt, 2.6512; C, 1.6476; N, 1.5651; H$_C$, 1.1880; H$_N$, 1.1605. Me$_2$Pt: outer, 5.5222; Pt, 2.6577; C, 1.6794; H, 1.2390. NH$_3$: outer, 2.7840; N, 1.5651; H, 1.1605. PH$_3$: outer, 3.4933; P, 2.2564; H, 1.3410. AsH$_3$: outer, 3.6760; As, 2.3907; H, 1.3890. CNH: outer, 3.1879; C, 1.6476; N, 1.5651; H, 1.1605. C$_2$H$_4$: outer, 4.1497; C, 1.6794; H, 1.2390.

Table II. Ionization Energies (eV) and Assignments for the Upper Valence Orbitals of the Complexes *cis*-$[PtMe_2(PR_3)_2]$

band	PMe_3	PMe_2Ph	$PMePh_2$	PEt_3	PMe $(OEt)_2$	$P(OMe)_3$	$P(OEt)_3$	$P(NMe_2)_3$	assgnt
A	7.34	7.17	7.12	7.23	7.48	7.72	7.55	6.82	$4a_1$
B	7.70	7.45	7.43	7.64	7.85	8.09	7.95	7.19	$2b_2$
C	7.98	7.82	7.73	8.04	8.16	8.40	8.27	7.57	$3a_1$
D	8.38	8.18	8.02	8.32	8.49	8.74	8.59	7.93	$1b_1$
E	8.80	8.83	8.65	8.70	9.06	9.30	9.13	8.49[a]	$1a_2$
F	9.08			8.97	9.38	9.62	9.52	9.12	$2a_1$
G,H		9.14, 9.48	9.05, 9.40						Ph (π_1 and π_2)

[a] Ligand band superimposed on this band; see text.

Table III. He II/He I Area Ratios for *cis*-$[PtMe_2L_2]$[a]

compd	A	B	C	D	E	F
L_2						
COD	1.00	0.82	1.05	0.90	1.05	1.01
NBD	1.00	0.66	1.03	1.04	1.04	1.10
TMED	1.00	0.90	0.93	0.77	0.77	0.82
L[b]						
PMe_3	1.00	0.81	0.87	1.08	0.83	0.89
PEt_3	1.00	0.83	0.90	0.88	0.82	1.10
$P(OMe)_3$	1.00	0.99	0.90	1.08	1.04	1.13
$P(OEt)_3$	1.00	0.84	0.96	1.14	1.18	1.10
$P(NMe_2)_3$	1.00	0.98	0.84	0.81	0.55	0.89
$AsMe_3$	1.00	1.05	1.02	1.12	1.00	0.88
CNMe	1.00	1.13	1.07	0.96	1.15	1.10

[a] The band A is used as a reference in the He I and He II area calculations. [b] For L = PMe_2Ph, $PMePh_2$, and CNPh, reliable He II spectra could not be obtained due to the low vapor pressure of these complexes below their decomposition temperatures.

Results and Discussion

General Features of the Spectra. Four typical spectra are shown in Figure 1. It is convenient to discuss the regions of the spectra in the energy ranges >10.5 eV and <10.5 eV separately. In the region >10.5 eV the spectra contain broad envelopes, which are fitted to the minimum number of bands but which contain contributions from ionizations of many ligand-based MO's as well as the lowest energy (largest IP) metal–ligand σ-MO's. The He II/HeI intensity ratio is much lower for these higher energy ionizations than for the bands at energies <10.5 eV, as expected for ligand-based ionizations. This region at >10.5 eV will not be discussed further.

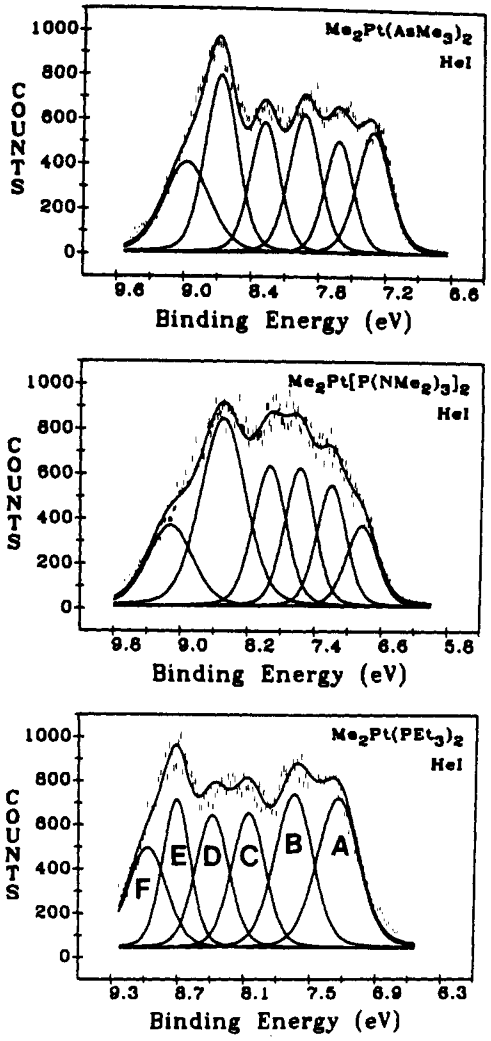

Figure 4. He I spectra of *cis*-$[PtMe_2L_2]$, where L = PEt_3, $P(NMe_2)_3$, and $AsMe_3$.

In the energy region <10.5 eV (Figures 2–4 and S1–S3 (supplementary material)), there are often six sharp resolved bands (Figures 2 and 4) though, for some ligands, extra ligand bands are present and, in some cases, two or more of the bands appear to be degenerate. A six-peak fit to the more poorly resolved spectra (e.g. Figure S2) (supplementary material) gives consistent line widths and areas and good overall fits. The ionization energy and intensity data are given in Tables I–III. Since a platinum(II) complex should have four filled 5d orbitals, two of the six bands must be due to metal–ligand σ-bond ionizations. It is interesting to note that the IE's for all levels (Tables I and II) are shifted by very similar amounts from one compound to another. For example, with the change from $[Me_2PtL_2]$ with L = $P(NMe_2)_3$ to L = MeNC, peaks A–F shift by 0.8, 0.8, 0.7, 0.8, 0.6, and 0.5 eV, respectively.

---

(20) For $Me_2Pt(PH_3)_2$, Pt–C = 2.120 Å, Pt–P = 2.285 Å, ∠C–Pt–C = 81.92°, and ∠P–Pt–P = 97.75° (Wisner, J. M.; Bartczak, T. J.; Ibers, A. *Organometallics* **1986**, *5*, 2044), C–H = 1.10 Å and ∠H–C–H = 109.5° (Chan, T. C. S. M.Sc. Thesis, University of Western Ontario, London, Canada, 1982, p 35), P–H = 1.415 Å (Kuchitzer, K. *J. Mol. Spectrosc.* **1961**, *7*, 399), and ∠H–P–H = 105° (Bartell, L. S.; Hirst, R. C. *J. Chem. Phys.* **1959**, *31*, 449). The same values of C–H, ∠H–C–H, and ∠C–Pt–C were also used in Me_2Pt and Me_2Pt_2 (L = NH_3, AsH_3, C_2H_4, CNH), and the same value of Pt–C was also used in Me_2Pt and Me_2PtL_2 (L = NH_3, AsH_3). For $Me_2Pt(NH_3)_2$, Pt–N = 2.09 Å and ∠N–Pt–N = 87.0° (Barber, M.; Clark, J. R.; Hinchliff, A. *J. Mol. Struct.* **1979**, *57*, 169), N–H = 1.03 Å and ∠H–N–H = 109.5° (Takahashi, M.; Watanabe, I.; Ikeda, S. *Bull. Chem. Soc. Jpn.* **1987**, *60*, 9). For $Me_2Pt(AsH_3)_2$, Pt–As = 2.435 Å, ∠As–Pt–As = 103.7°, and ∠H–As–H = 102.9° (Russell, D. R.; Tucker, P. A. *J. Chem. Soc., Dalton Trans.* **1975**, 1752) and As–H = 1.511 Å (Dobbs, K. D.; Hehre, W. J. *J. Comput. Chem.* **1986**, *7*, 359). For $Me_2Pt(C_2H_4)_2$, $Pt{-}C_{Me}$ = 2.068 Å, Pt–ol = 2.169 Å, and ∠ol–Pt–ol = 91.25° (ol = midpoint of C=C bond. Day, C. S.; Day, V. W.; Shaver, A.; Clark, H. C. *Inorg. Chem.* **1981**, *20*, 2188), and C=C = 1.375 Å, C–H = 1.087 Å, ∠H–C–H = 114.9°, and $\angle H{-}C_1{-}C_2$ = 121.08° (Love, R. A.; Koetzle, T. F.; Williams, G. J. B.; Andrews, L. C.; Bau, R. *Inorg. Chem.* **1975**, *14*, 2653); the same value of $Pt{-}C_{Me}$ was also used in $Me_2Pt(CNH)_2$. For $Me_2Pt(CNH)_2$, $Pt{-}C_N$ = 1.86 Å and C≡N = 1.19 Å (Scrivanti, A.; Carturan, G.; Belluco, U.; Brescianipahor, N.; Calligaris, M.; Randaccio, L. *Inorg. Chim. Acta* **1976**, *20*, L3), $\angle C_N{-}Pt{-}C_N$ = 91° (Jovanovič, B.; Manojlovič-Muir, L.; Muir, K. W. *J. Chem. Soc., Dalton Trans.* **1972**, 1178), and N–H was the same as in $Me_2Pt(NH_3)_2$. For NH_3, N–H = 1.008 Å and ∠H–N–H = 107.3° (*Handbook of Chemistry and Physics*; CRC Press: Cleveland, OH, 1981). For PH_3, P–H = 1.415 Å and ∠H–P–H = 93.45° (Norman, J. G., Jr. *J. Chem. Phys.* **1974**, *61*, 4630). For AsH_3, As–H = 1.511 Å and ∠H–As–H = 92.1° (Dobbs, K. D.; Hehre, W. J. *J. Comput. Chem.* **1986**, *7*, 359). For C_2H_4, C=C = 1.337 Å, C–H = 1.086 Å, ∠H–C–H = 117.3°, and $\angle H{-}C_1{-}C_2$ = 121.4° (Roberts, J. D.; Caserio, M. C. *Basic Principles of Organic Chemistry*, 2nd ed.; 1977, W. A. Benjamin, Inc.: Reading, MA, 1977). For CNH, the geometries were used as in $Me_2Pt(CNH)_2$.

Table IV. MS–Xα Results for *cis*-[PtMe$_2$] Upper Valence Orbitals

orbital	orbital energy, eV	charge distribution,[a] % Pt	C	H	inter	outer
4a$_1$	2.06	4 s, 9 p$_z$, 5 d$_{z^2}$	9		41	32
2b$_2$	2.09	11 p$_y$, 21 d$_{yz}$	23	2	32	10
3a$_1$	5.26	15 s, 1 p$_z$, 40 d$_{x^2-y^2}$	11	1	29	3
2a$_1$	5.90	85 d$_{z^2}$	1	3	10	1
1a$_2$	5.94	87 d$_{xy}$	1	2	9	1
1b$_1$	5.98	86 d$_{xz}$	1	2	10	1
1a$_1$	7.71	6 s, 2 p$_z$, 44 d$_{x^2-y^2}$	30	4	12	2
1b$_2$	8.20	1 p$_y$, 58 d$_{yz}$	27	5	7	2

[a] The contributions of carbon are essentially 2p character. For the Pt contributions, the % contribution followed by the orbital is given. The particular p or d orbital is not given by the calculation directly, and the assignment of, for example, an a$_1$ orbital to mostly d$_{z^2}$ or d$_{x^2-y^2}$ is based on the orbital contour diagrams. These assignments are therefore not certain.

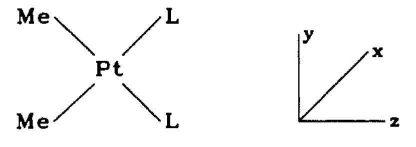

L=PMe$_3$, PMe$_2$Ph, PMePh$_2$, PEt$_3$, P(NMe$_2$)$_3$,
PMe(OEt)$_2$, P(OEt)$_3$, P(OMe)$_3$, AsMe$_3$
CNMe and CNPh

or

L$_2$=Me$_2$NCH$_2$CH$_2$NMe$_2$(TMED),
1,5-cyclooctadiene(COD) and norbornadiene(NBD)

Figure 5. Structure of the molecules with the axis system used in the text.

For transition-metal complexes it is often possible to distinguish between d orbitals and σ orbitals by comparing the band intensities in the He I and He II photoelectron spectra, since d orbitals frequently have a greater relative photoionization cross section for He II radiation.[9,21] However, as the data in Table III indicate, the six low-energy bands in the photoelectron spectra often give very similar He II/He I band intensity ratios, and so this technique is not useful for these dimethylplatinum(II) complexes. Possible reasons for the similar He II/He I ratios in platinum compounds are discussed in our recent papers.[10,22]

Two methods have proved useful for band assignment. First, it was observed that the lowest ionization energy band, labeled band A, was split into two peaks for the complexes *cis*-[PtMe$_2$L$_2$] with L$_2$ = COD, NBD, and TMED[10] (Figures 2 and 3) and this splitting was assigned to vibrational coupling with C═C or N—C stretching modes of the coordinated ligands. In turn, this indicates that the HOMO must have metal–ligand σ character. Second, MS–Xα calculations were carried out on the model compounds *cis*-[PtMe$_2$L$_2$], where L = NH$_3$, PH$_3$, AsH$_3$, C$_2$H$_4$, and NH≡C. These calculations, in agreement with a previous calculation for *cis*-[PtMe$_2$(PPh$_3$)$_2$],[2] also predict that the HOMO is a metal–ligand σ orbital. Further details of the calculations and spectral assignments are given below.

Molecular Orbital Calculations. (a) Complex *cis*-[PtMe$_2$(C$_2$H$_4$)$_2$]. In order to draw up an energy correlation diagram, the molecules *cis*-[PtMe$_2$L$_2$] (Figure 5, including the definition of axes) have been considered to be formed by combination of the fragments *cis*-[PtMe$_2$] and L$_2$, and calculations have been carried out for each species. There is a previous MS–Xα calculation by Johnson and co-workers on *cis*-[PtMe$_2$(PH$_3$)$_2$] in which the alternative approach was used, considering the molecule to be formed from *cis*-[Pt(PH$_3$)$_2$] and two methyl radicals; the results of the two calculations for this molecule are in good agreement.[2] In the correlation diagram of Figure 6 for *cis*-[PtMe$_2$(C$_2$H$_4$)$_2$], only the interactions between the Me$_2$Pt orbitals and the outer orbitals of the ligands C$_2$H$_4$ are considered for the sake of simplicity.

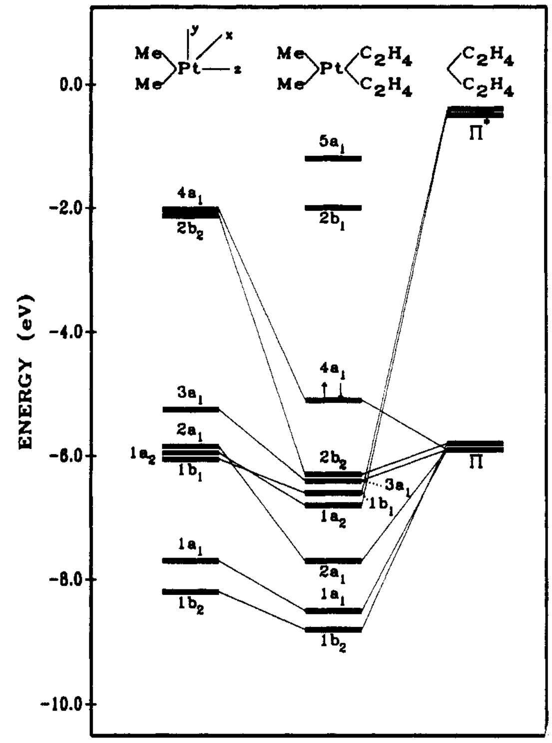

Figure 6. Orbital interaction diagram for *cis*-[PtMe$_2$(C$_2$H$_4$)$_2$].

Consider first the fragment *cis*-PtMe$_2$. There are two σ-bonding MO's, the orbitals 1b$_2$ and 1a$_1$, in Figure 6 and in Table IV. . Orbital 1b$_2$ is formed mostly by overlap of 5d$_{yz}$ on platinum with the antisymmetric combination of the two Me σ orbitals, while the orbital 1a$_1$ is formed by the overlap of 6s, 5d$_{x^2-y^2}$ on platinum with the symmetric combination of the two Me σ orbitals, shown as follows:

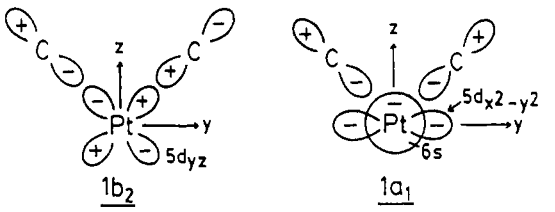

There are two virtual orbitals also, labeled 2b$_2$ and 4a$_1$, which arise mostly from the antibonding combination of the methyl 1a$_1$ and 1b$_2$ orbitals with the metal d orbitals. The orbital 2b$_2$ is formed by the symmetric combination of the two CH$_3$ σ orbitals bonding to 6p$_y$ but antibonding to 5d$_{yz}$ on platinum. The net result is weakly antibonding because of its higher 5d$_{yz}$ character. The orbital 4a$_1$ is very diffuse because of small atomic contributions from both the platinum atom and methyl groups (Table IV).

---

(21) Bancroft, G. M.; Chan, T.; Puddephatt, R. J. *Inorg. Chem.* **1982**, *22*, 2133. Bancroft, G. M.; Chan, T.; Puddephatt, R. J.; Tse, J. S. *Inorg. Chem.* **1982**, *21*, 2946.

(22) Yang, D. S.; Bancroft, G. M.; Puddephatt, R. J.; Bursten, B. E.; McKee, S. D. *Inorg. Chem.* **1989**, *28*, 872.

Table V. MS-Xα Results for *cis*-$[PtMe_2(C_2H_4)_2]$ Upper Valence Orbitals

orbital	orbital energy, eV	trans-state energy, eV	charge distribution, % Pt	C_{Me}	$C_{C=C}$	H_{Me}	$H_{C=C}$	inter	outer
$4a_1$	5.09	7.57	3 s, 6 p_z, 24 d_{z^2}	16	24	1	1	23	2
$2b_2$	6.34	8.73	8 p_y, 1 d_{yz}	10	47	2		31	1
$3a_1$	6.38	8.93	11 s, 48 $d_{x^2-y^2}$	7	8	2	1	22	1
$1b_1$	6.56	9.22	78 d_{xz}	2	5	3	4	8	
$1a_2$	6.78	9.41	66 d_{xy}	2	11	3	9	8	
$2a_1$	7.73	10.30	1 s, 55 d_{z^2}	4	18	4		18	
$1a_1$	8.49	11.06	4 s, 45 $d_{x^2-y^2}$	21	11	4	1	12	1
$1b_2$	8.78	11.36	49 d_{yz}	21	13	4	4	8	1

Table VI. MS-Xα Results for *cis*-$[PtMe_2(PH_3)_2]$ Upper Valence Orbitals

orbital	orbital energy,[a] eV		trans-state energy, eV	charge distribution, % Pt	C	P	H_C	H_P	inter	outer
$4a_1$	4.60	4.70	7.24	6 s, 10 p_z, 10 d_{z^2}	34	8	3	2	22	5
$2b_2$	5.13	5.27	7.76	11 p_y, 3 d_{yz}, 2 f	24	22	2	3	33	
$3a_1$	5.39	5.37	7.91	9 s, 46 $d_{x^2-y^2}$	1	17		3	22	2
$1b_1$	6.02	5.86	8.52	86 d_{xz}	1	1	2	2	8	
$1a_2$	6.09	5.94	8.60	85 d_{xy}	1	2	2	2	8	
$2a_1$	6.16	6.05	8.69	77 d_{z^2}	4	5	3	3	7	1
$1a_1$	8.28	8.40	10.94	9 s, 39 $d_{x^2-y^2}$	8	27	1	6	7	3
$1b_2$	8.95	9.01	11.64	52 d_{yz}	10	23	4	5	6	

[a] The first column is the nonrelativistic result, and the second column is the relativistic result.

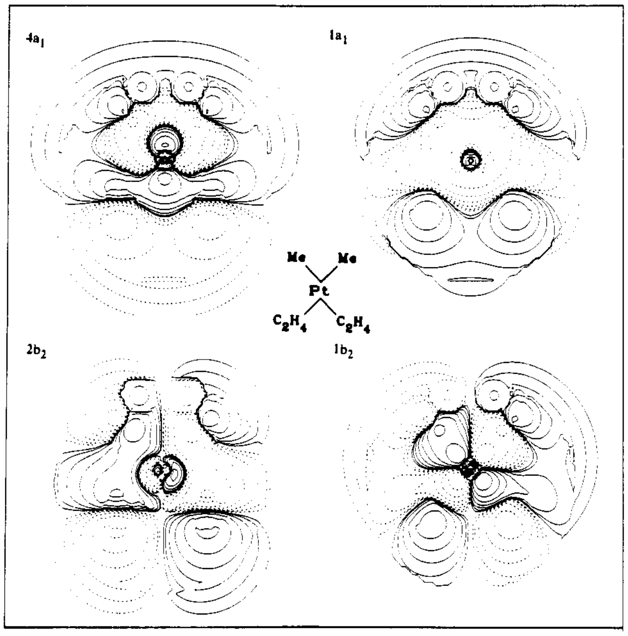

Figure 7. Contour diagrams of orbitals $4a_1$, $2b_2$, $1a_1$, and $1b_2$. The contours are plotted on the *yz* plane and at values of ±0.002, ±0.0047, ±0.0094, ±0.0188, ±0.0375, and ±0.150 e bohr^{-3}, starting from the outermost.

Between these $PtMe_2$ σ and virtual levels, there are four nonbonding orbitals having mostly platinum 5d character, as expected for a platinum(II) d^8 complex. These are identified as $3a_1$ ($d_{x^2-y^2}$, HOMO), $2a_1$ (d_{z^2}), $1a_2$ (d_{xy}), and $1b_1$ (d_{xz}), using the axes defined in Figure 5. The orbital $3a_1$ is at highest energy because of its involvement in PtMe bonding as described above, which gives it some σ^* character.

Now the orbitals of interest for the *cis*-$(C_2H_4)_2$ ligands are the π orbitals ($a_1 + b_2$ symmetry) and the π^* orbitals ($a_2 + b_1$ symmetry) arising from the C=C bonds. The energies of these MO's, as calculated by the MS-Xα method, are shown in Figure 6. It is clear from the resulting correlation diagram that there is strong mixing of the π levels of C_2H_4 with the σ ($1a_1 + 1b_2$) and virtual ($4a_1 + 2b_2$) orbitals of the Me_2Pt fragment and also with the platinum d orbitals ($2a_1 + 3a_1$) of a_1 symmetry. The $2a_1$ orbital is particularly stabilized by this interaction (Figure 6). It is possible to identify the σ orbitals and d orbitals in Figure 6 from their origins, but these characters are strongly mixed in some of the MO's. The calculated orbital characters for this complex are given in Table V.

There are two strongly bonding σ MO's labeled $1a_1$ and $1b_2$ and two weakly bonding σ MO's labeled $2b_2$ and $4a_1$. Contour diagrams for these orbitals are given in Figure 7. The HOMO is $4a_1$, which is fairly evenly distributed between platinum, methyl, and ethylene character (Table V) but retains the Pt–Me character of the $PtMe_2$ fragment along with Pt–C_2H_4 σ character, as indicated by the contour diagram of Figure 7. The orbital $2b_2$ is calculated to have very largely the character of the C=C π orbital from which it is derived (Table V and Figures 6 and 7).

Now considering the platinum 5d orbitals of the Me_2Pt fragment, it has been seen that the $3a_1$ and, especially, the $2a_1$ orbitals are strongly stabilized by taking on C_2H_4 π character in forming the complex *cis*-$[PtMe_2(C_2H_4)_2]$. The orbitals $1a_2$ and $1b_1$ are also stabilized by interacting with the C_2H_4 π^* orbitals of appropriate symmetry. This is the back-bonding expected in this type of complex, but it is relatively weak, since the C_2H_4 π^* level is at high energy.

To summarize, the calculation for *cis*-$[PtMe_2(C_2H_4)_2]$ predicts that the upper eight occupied MO's will contain four orbitals of mostly platinum 5d character sandwiched between two strongly bonding σ MO's and two weakly bonding σ MO's.

(b) Complexes *cis*-$[PtMe_2(EH_3)_2]$, E = N, P, or As. The results for these complexes are similar to those for *cis*-$[PtMe_2(C_2H_4)_2]$ (Tables VI and S1 and S2 (supplementary material)) and so are treated more briefly. The calculations on the free ligands EH_3 indicate that the lone-pair orbitals of symmetry $a_1 + b_2$ have mostly p character with s contributions of 7% in NH_3, 19% in PH_3, and 20% in AsH_3. No virtual orbital was found for NH_3 in an energy search up to −0.007 eV, and the virtual orbitals for PH_3 (−0.38 eV) and AsH_3 (−0.54 eV) are contributed largely from outer-sphere regions and thus are not shown in the correlation diagram (Figure 8).

Compared to those of *cis*-$[PtMe_2(C_2H_4)_2]$, the σ orbitals of EH_3 interact more strongly with the $1b_2$ and $1a_1$ levels and less strongly with the $4a_1$ and $2b_2$ levels of the *cis*-$[PtMe_2]$ fragment. This leads to a larger calculated energy gap between $1b_2$ and $2b_2$ or $1a_1$ and $4a_1$ for the EH_3 complexes. In addition, the orbitals $3a_1$, $2a_1$, $1a_2$, and $1b_1$ of the Me_2Pt fragment, which were identified earlier as having mostly platinum 5d character, are much less strongly perturbed by the additional bonding to the EH_3 groups compared to C_2H_4. This is easily seen by comparison of the correlation diagrams in Figures 6 and 8. Both σ and π interactions with the EH_3 groups are calculated to be lower than with C_2H_4 in all cases,

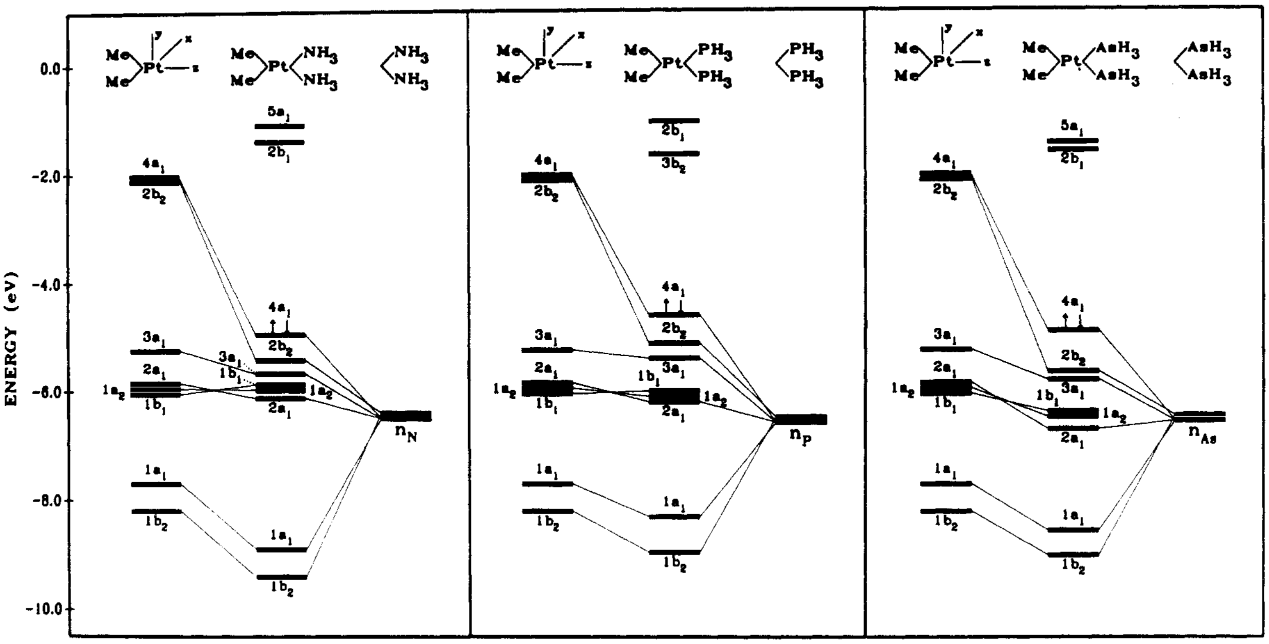

Figure 8. Orbital interaction diagram for *cis*-[$PtMe_2(EH_3)_2$], where E = N, P, and As.

but both σ and π bonding involving these d orbitals on platinum follow the series $EH_3 = AsH_3 > PH_3 > NH_3$. In all cases, however, the orbitals identified as having mostly Pt 5d character are sandwiched between two strongly bonding σ MO's and two nonbonding or weakly bonding σ MO's, similar to the case of *cis*-[$PtMe_2(C_2H_4)_2$].

Finally, it should be pointed out that the relativistic and nonrelativistic orbital energies are very similar indeed (Table VI). Thus, as has been shown for other square-planar platinum(II) complexes,[9] relativistic corrections are very small.

(c) Complex *cis*-[$PtMe_2(C{\equiv}NH)_2$]. The results for this complex are given in Table S3 (supplementary material) and Figure 9. This is the most complex example studied, since the HN≡C ligands have both π_x and π_y filled orbitals and π_x* and π_y* empty orbitals of energy suitable for bonding, as well as the σ lone-pair orbitals.

The σ lone-pair orbitals of HNC are sp hybrid MO's and are of low energy, so that they interact very strongly with the $1a_1$ and $1b_2$ orbitals of the Me_2Pt fragment and only weakly with the $4a_1$ and $2b_2$ orbitals. The HNC ligands appear to act mostly as π-acceptor (rather than π-donor) ligands, but the π_x orbitals are stabilized to some extent on coordination of HNC, and this suggests that the isocyanide can also act as a weak π donor.

Finally, we note that the σ-orbital $3b_2$ in *cis*-[$PtMe_2(HNC)_2$], which correlates with the $2b_2$ orbital of the *cis*-[$PtMe_2$] fragment, is calculated to be almost degenerate with three of the platinum d orbitals. In the other complexes studied, the corresponding orbital was always calculated to lie higher in energy than the 5d orbitals.

Spectral Assignment and Interpretation. (a) Complexes [$PtMe_2(COD)$] and [$PtMe_2(NBD)$]. The low-IE regions of the spectra for these compounds are similar and contain six well-resolved bands, as shown in Figure 2. Five of these bands (B–F in Figure 2) could be fitted to single Lorentzian–Gaussian band shapes. However band A was clearly split into two peaks with separations of 0.17 eV (~1400 cm^{-1}) for [$PtMe_2(COD)$] and 0.15 eV (~1200 cm^{-1}) for [$PtMe_2(NBD)$]. The area of band A is approximately equal to the areas of each of the other five bands B–F, suggesting that the splitting is not due to overlap of peaks arising from two almost degenerate MO's.[23] More importantly, the splittings correlate well with the known C=C stretching frequencies of 1428 cm^{-1} in [$PtMe_2(COD)$] and 1174–1188 cm^{-1} in [PtIMe(NBD)],[24] and the MS-Xα calculated transition-state energies predict that the $4a_1$ and $2b_2$ orbitals should be well separated (Table V). Therefore, the splitting is assigned to vibrational coupling and indicates that the HOMO has substantial platinum–alkene bonding character, as predicted by the MS-Xα calculation on the model compound *cis*-[$PtMe_2(C_2H_4)_2$]. Although resolution of ligand vibrational splitting is not common, CO vibrational structure has also been seen on the bands due to metal–carbon σ-MO ionizations in [$W(CO)_6$].[25]

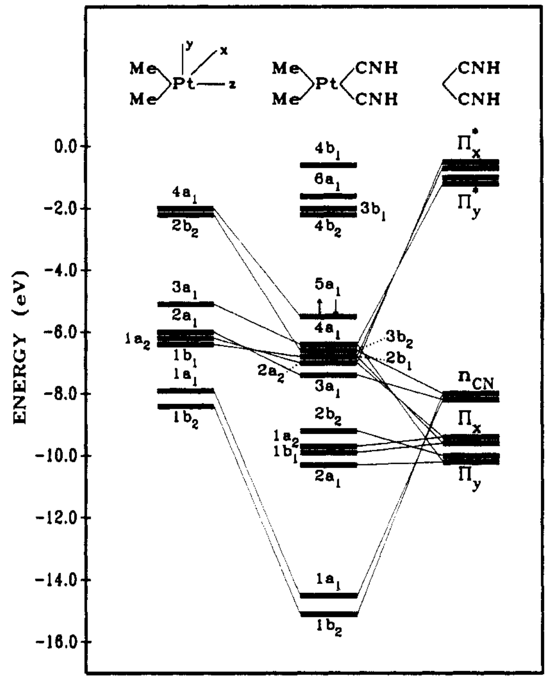

Figure 9. Orbital interaction diagram for *cis*-[$PtMe_2(CNH)_2$].

Band B is assigned to a second metal–ligand σ MO for the following reasons. First, the MS-Xα calculation for *cis*-

---

(23) Eland, J. H. D. *Photoelectron Spectroscopy*, 2nd ed.; Butterworth & Co. Ltd.: London, 1984.

(24) Kistner, C. R.; Hutchinson, J. H.; Doyle, J. R.; Storlie, J. C. *Inorg. Chem.* **1963**, *2*, 1255. Appleton, T. G.; Hall, J. R.; Neale, D. W.; Williams, M. A. *J. Organomet. Chem.* **1984**, *276*, C73. Clark, H. C.; Manzer, L. E. *J. Organomet. Chem.* **1973**, *59*, 411. Chisholm, M. H.; Clark, H. C.; Manzer, L. E.; Stothers, J. B.; Ward, J. E. H. *J. Am. Chem. Soc.* **1975**, *97*, 721.

(25) Higginson, B.; Lloyd, D. R.; Burroughs, P.; Gibson, D. M.; Orchard, A. F. *J. Chem. Soc., Faraday Trans. 2* **1973**, *69*, 1659. Hubbard, J. L.; Lichtenberger, D. L. *J. Am. Chem. Soc.* **1982**, *104*, 2132.

[$PtMe_2(C_2H_4)_2$] suggests this assignment and also predicts that the orbital has largely alkene π character. In agreement, band B gives the lowest He II/He I band intensity ratio for any of the bands A–F for both [$PtMe_2$(COD)] and [$PtMe_2$(NBD)] (Table III), suggesting much ligand character in this MO. Vibrational splitting of the band would be expected but was not resolved, probably because of strong overlap with band C (Figure 2).

It is then natural to assign the next four bands (C–F) to ionizations from orbitals with mostly Pt 5d character. There is no experimental evidence to aid assignment of each band to a specific d orbital, and so the assignments in Table I are based only on the predictions of the MS–Xα calculation. They are therefore tentative assignments only. The MS–Xα calculation predicts that the two strongly bonding σ MO's $1a_1$ and $1b_2$ of Figure 6 should lie at high ionization energy and the peaks from these MO's are presumed to be hidden in the broad envelope at ~11 eV.

Consider next the energy shift of the alkene π orbitals on coordination. Free COD shows one π-ionization band at 9.06 eV,[26] and NBD gives two bands at 8.69 and 9.55 eV.[27] In the complex [$PtMe_2$(COD)], the σ orbitals having the most character of the alkene π orbitals are $4a_1$ and $2b_2$, which appear in the photoelectron spectra at 7.76/7.93 and 8.47 eV, respectively. The corresponding calculated energies for *cis*-[$PtMe_2(C_2H_4)_2$] are 7.57 and 8.73 eV, after allowance for relaxation effects. It is important to note that Figure 6, and the other correlation diagrams, refer to the ground state only. The calculated and observed ionization energies for the C_2H_4 π orbital are 9.66 and 10.51 eV,[28] respectively. Thus it appears that the π orbitals are destabilized on coordination and it is therefore tempting to suggest that the major component of the Pt–alkene bonding is the back-bonding, which increases the charge on the alkene.[29–32] However, this conclusion is not justified, since the MO's for *cis*-[$PtMe_2(C_2H_4)_2$] are delocalized and there is much C_2H_4 π character calculated for the low-energy MO's $1b_2$, $1a_1$, and $2a_1$. Similar considerations apply to the other complexes *cis*-[$PtMe_2L_2$], as described below. The best evidence for back-bonding in *cis*-[$PtMe_2(C_2H_4)_2$] and *cis*-[$PtMe_2$(COD)] from the present work is the stabilization of the d_π orbitals $1b_1$ and $1a_2$ of the Me_2Pt fragment on coordination of ethylene ligands as predicted by the MS–Xα calculation (Figure 6), coupled with the excellent agreement between the experimentally observed band energies for *cis*-[$PtMe_2$(COD)] and the calculated band energies for *cis*-[$PtMe_2(C_2H_4)_2$] (Tables I and V).

(b) Complex [$PtMe_2$(TMED)]. The spectra in the low-IE region are displayed in Figure 3, in which five resolved bands are observed. Band A again splits into two peaks with a separation of 0.13 eV. This corresponds to the N–C stretching frequency of ~1100 cm^{-1},[33] and the splitting is therefore attributed to vibrational coupling. In this case the assignment is tentative because the calculation on the model compound *cis*-[$PtMe_2(NH_3)_2$] indicates only a low contribution of N-orbital character to the HOMO $4a_1$. However, the model is a crude one and the calculations on the other molecules *cis*-[$PtMe_2L_2$] do indicate substantial L-orbital character in the HOMO. To see N–C vibrational coupling, the nitrogen lone-pair orbital must be delocalized to some extent onto the carbon atoms of the ligand TMED, which is indeed evidenced in $N(CH_3)_3$ by electron momentum spectroscopy.[34]

The fourth band in the photoelectron spectrum (labeled D, E) has about twice the area of the other bands and is therefore assigned as due to two almost degenerate MO's. Because TMED has no π-acceptor properties, the platinum d_π orbitals d_{xz} ($1b_1$) and d_{xy} ($1a_2$) are expected to be close in energy, and the calculation also predicts near degeneracy of these levels. The band D,E is therefore assigned to these orbitals, and the other bands are assigned in a similar way as for *cis*-[$PtMe_2(C_2H_4)_2$].

(c) Complexes *cis*-[$PtMe_2(ER_3)_2$]. This is the largest group of compounds studied, with ER_3 = PMe_nPh_{3-n} (n = 1–3), PEt_3, $P(NMe_2)_3$, $PMe(OEt)_2$, $P(OMe)_3$, $P(OEt)_3$, and $AsMe_3$. The compounds were designed to give as wide a range of electronic properties of the phosphine and related ligands as possible, while accommodating the requirement of high volatility (without decomposition) needed to obtain satisfactory photoelectron spectra. The spectra are given in Figures 4 and S1 and S2 (supplementary material), and the data are in Table II.

The spectra are less resolved than those for the complexes discussed above, but in most cases the spectra were fitted most satisfactorily with six bands. Two extra bands, G and H, were present in the spectra of the complexes with phenylphosphines $PMePh_2$ and PMe_2Ph and are readily assigned as due to phenyl π-electron ionizations.[35] In no case does band A show resolved vibrational structure, in contrast to the observations for the alkene and TMED complexes discussed above. Such splittings are not expected, since the characteristic ν(PC), ν(PO), ν(PN), or ν(AsC) frequencies are too small to give resolved fine structure. For many of the compounds bands A and B are also close in energy and fairly broad, which would make vibrational splittings difficult to resolve.

The platinum d_π orbitals are the $5d_{xz}$ ($1b_1$) and $5d_{xy}$ ($1a_2$). These are expected to be almost degenerate, and the calculations on the model compounds *cis*-[$PtMe_2(PH_3)_2$] and *cis*-[$PtMe_2(AsH_3)_2$] (Tables VI and S2 (supplementary material) and Figure 8) predict that they are close in energy with $1a_2$ at slightly lower energy than $1b_1$, presumably due to slightly better back-bonding to phosphorus or arsenic π-acceptor orbitals by the $5d_{xy}$ orbital (note that $1a_2$ and $1b_1$ should be degenerate if all angles were 90°, but a typical P–Pt–P angle is ca. 97°). From these arguments, bands D and E are assigned to the $1b_1$ and $1a_2$ levels, and it is particularly interesting that the energy gap between these orbitals is greater for the phosphorus donors with more electronegative substituents RO, R_2N, or Ph than with methyl or ethyl substituents. This is fully consistent with the expected stronger back-bonding for these ligands with electronegative substituents[36,37] and supports the assignment. It was noted earlier that in the TMED complex, with no back-bonding ability, bands D and E are degenerate.

Finally, in the complex *cis*-[$PtMe_2\{P(NMe_2)_3\}_2$] it was found that band E was about double the intensity of other bands and that its intensity was much reduced in the He II spectrum. An ionization of ligand electrons is expected in this region due to the σ orbital of two nitrogen lone pairs interacting in an antisymmetric fashion[38] and is presumed to overlap with the platinum d_π band, which is also expected. The assignments are given in Table II.

(d) Complexes *cis*-[$PtMe_2(C{\equiv}NR)_2$], R = Me or Ph. The spectrum of *cis*-[$PtMe_2(C{\equiv}NMe)_2$] (Figure S3 (supplementary material)) is typical of the complexes *cis*-[$PtMe_2L_2$], and ionization data are given in Table II. In the absence of other useful information, the tentative band assignments given in Table II are those predicted by the calculation on the model compound *cis*-[$PtMe_2(C{\equiv}NH)_2$]. In this complex, the HOMO $5a_1$ (Figure 9) is predicted to contain almost no isocyanide ligand character and so vibrational fine structure is not expected.

The photoelectron spectrum of *cis*-[$PtMe_2(PhNC)_2$] (Figure S3 (supplementary material)) is different in two respects. First,

---

(26) Batich, C.; Ermer, O.; Heilbronner, E. *J. Electron Spectrosc. Relat. Phenom.* **1973**, *1*, 333.

(27) Plamer, M. H. *J. Mol. Struct.* **1987**, *161*, 333.

(28) Turner, D. W.; Baker, C.; Baker, A. D.; Brundle, C. B. *Molecular Photoelectron Spectroscopy*; Wiley-Interscience: New York, 1970.

(29) Calabro, D. C.; Lichtenberger, D. L. *J. Am. Chem. Soc.* **1981**, *103*, 6846.

(30) Morelli, G.; Polzonetti, G.; Sessa, V. *Polyhedron* **1985**, *4*, 1185.

(31) Cook, C. D.; Wan, K. Y.; Gelius, U.; Humrin, K.; Johansson, G.; Olsson, E.; Siegbahn, H.; Nordling, C.; Siegbahn, K. *J. Am. Chem. Soc.* **1971**, *93*, 1904.

(32) Kitaura, K.; Sakaki, S.; Morokuma, K. *Inorg. Chem.* **1981**, *20*, 2292. Sakaki, S.; Kudou, N.; Ohyoshi, A. *Inorg. Chem.* **1977**, *16*, 202.

(33) Rao, C. N. R. *Chemical Applications of Infrared Spectroscopy*; Academic Press Inc. Ltd.: London, 1963; p 250.

(34) Bawagan, A. O.; Brion, C. E. *Chem. Phys.* **1988**, *123*, 51.

(35) Puddephatt, R. J.; Bancroft, G. M.; Chan, T. *Inorg. Chim. Acta* **1983**, *73*, 83.

(36) Yarbrough, L. W., II; Hall, M. B. *Inorg. Chem.* **1978**, *17*, 2269.

(37) Yamamato, A. *Organotransition Metal Chemistry*; John Wiley & Sons, Inc.: New York, 1986; p 209.

(38) Gonbeau, D.; Sanchez, M.; Guillouzo, G. P. *Inorg. Chem.* **1981**, *20*, 1966 and references therein.

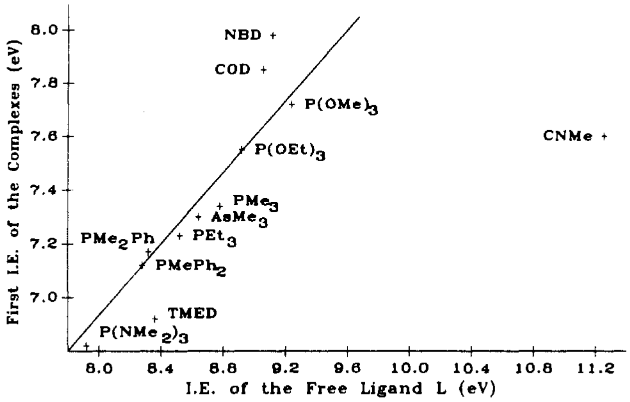

Figure 10. Graph of the first IE (eV) of the complex *cis*-[$PtMe_2L_2$] vs the IE (eV) of the ligand L.

there are two bands at 9.91 and 10.57 eV, which are readily assigned as due to phenyl π orbitals by analogy with the spectra of the free ligand and the complexes [$Fe(CO)_4(C{\equiv}NPh)$] and [$W(CO)_5(C{\equiv}NPh)$].[39-41] Second, the first band at 8.16 eV, which is narrow (fwhm = 0.5–0.6 eV) and can be fitted to only one band, appears to correspond to the first four bands of *cis*-[$PtMe_2(C{\equiv}NMe)_2$], which are resolved and spread over an energy range of >1 eV. The mean energies are then similar and indicate similar overall donor strength for MeNC and PhNC, as observed in other complexes.[39-41] Calculations on ligands $RN{\equiv}C$ have indicated that, when R = Ph compared to alkyl, the π^* level is stabilized and the π level is destabilized, thus leading to better energy matching with metal d orbitals.[42] It is then likely that there are differences in the π-donor and π-acceptor behavior of the $PhN{\equiv}C$ compared to $MeN{\equiv}C$ ligand, which lead to the major differences in the observed spectra. In particular the resolution of band E, due to the $5d_{xy}$ level, for *cis*-[$PtMe_2(C{\equiv}NPh)_2$] indicates that here back-bonding ($5d_{xy}$–π_x^*) may be significant in this complex, while the overlap of other bands may be due to enhanced π-donor interactions of PhNC.

Trends in Ligand Bonding. (a) σ-Donor Ability. Figure 10 shows a graph of the first ionization energy of the complex *cis*-[$PtMe_2L_2$] vs the ionization energy of the ligand L. Most of the ligands are phosphorus or arsenic donors, and for these there is an excellent correlation.[36,43,44] Similar correlations are observed for the other energy levels. This indicates that the ionization energy of such ligands is indeed a good criterion of donor strength. Interestingly, the ligand $P(NMe_2)_3$ also fits the correlation even though the ionization of the free ligand probably does not arise from the phosphorus lone-pair orbital.[38,45] The strong σ-donor ability of $P(NMe_2)_3$ has also been observed in the derivative *cis*-[$Mo(CO)_4L_2$].[44] We note also that, for the ligands PMe_nPh_{3-n}, the ionization energies of both the free ligands and the dimethylplatinum(II) complexes follow the series PMe_3 > PMe_2Ph > $PMePh_2$, the reverse of the series expected on electronegativity grounds. Similar effects have been observed previously with other metal complexes, and these results suggest that, in the gas phase, the phenylphosphines are the stronger donors. However, in solution the opposite trend appears to operate.[21,35,41,44-46]

If there is a synergic σ-donor/π-acceptor type of bonding in these complexes, then the ionization energies of the complexes may also be influenced to some extent by π-bonding effects. For example, TMED appears to be a stronger donor than predicted by the IE of the free ligand (Figure 10), and this may be due to the absence of π-acceptor properties for this ligand compared to the phosphorus donors. Similarly, COD and NBD appear as poorer donors than expected (Figure 10), and this could be due to their better π-acceptor properties compared to the phosphorus donors. Of course, these deviations from the correlation of Figure 10 could also be due to differences in the nature of the donor orbital of the ligand, which becomes progressively larger and more diffuse on going from nitrogen to phosphorus to alkene donors.

Finally, we note the very large deviation from the correlation of Figure 10 for the isocyanide ligands, which appear to be good donors though the ligand ionization energies are high. The π-donor ability of these ligands may be a factor here, but the deviation is probably too large to be explained solely by this effect.

If the ligands are arranged in order of the ionization energies for *cis*-[$PtMe_2L_2$], the donor series is $P(NMe_2)_3$ > TMED > $PMePh_2$ ~ PMe_2Ph > PEt_3 > $AsMe_3$ ~ PMe_3 > $PMe(OEt)_2$ > $P(OEt)_3$ > MeNC > $P(OMe)_3$ > COD > NBD > PhNC. Generally, this order is consistent with the σ-donor series determined by other methods though, as mentioned above, there are some reversals on going from the gas phase to solution.[46] The position of the isocyanide ligands in this series probably results from both σ and π effects.

(b) π-Acceptor Ability. As discussed earlier, the π-acceptor ability of the ligands may be measured by the splitting between the platinum $5d_\pi$ levels, that is the energy between bands D and E in the photoelectron spectra. There are problems in measuring this small energy difference accurately, but it is possible to arrange the ligands into three groups of decreasing π-acceptor properties on this basis. The series is $PMePh_2$, PMe_2Ph, $P(OMe)_3$, $P(OEt)_3$, $PMe(OEt)_2$, $P(NMe_2)_3$ > $AsMe_3$, PMe_3, PEt_3, COD, NBD > TMED. The series should be regarded with caution, but the general trend is reasonable.[46] Thus, the alkylphosphines or -arsines appear to be weaker π acceptors than the phosphorus donors with more electronegative substituents, and TMED has no π-acceptor properties on the basis of this criterion. The series may underestimate the π-acceptor ability of the alkene ligands however, since both the MS-Xα calculation and the deviation of COD and NBD from the correlation of Figure 10 suggest that the alkenes are better π acceptors than phosphines. The isocyanides are difficult to treat here because they appear to act both as π donors and π acceptors.

Implications for the Chemistry of the Complexes. These complexes may be considered as models for square-planar d^8 complexes generally; such complexes have a very rich chemistry and many have important catalytic applications. They are able to interact with both nucleophilic (by using the empty p orbital, $6p_x$ from the nomenclature of Figure 5, $6p_z$ from the more usual axes for square-planar complexes) and electrophilic reagents (by using the filled d orbital, $5d_{x^2-y^2}$ from Figure 2 axes, $5d_{z^2}$ from the more usual axes).

How can a knowledge of the energies of the molecular orbitals aid in interpreting reactivity? In oxidative addition chemistry of dimethylplatinum(II) compounds, it is clearly the filled d orbitals on the platinum that lead to metal-based nucleophilicity. The orbital used is $3a_1$, which is not the HOMO according to our interpretation of the spectra and the calculations but which is close enough to act as a nucleophile. The platinum–ligand σ-bonding MO $4a_1$ is the HOMO, but it is much more delocalized and inaccessible than the non-bonding platinum 5d orbital $3a_1$, and it is therefore reasonable that the more exposed orbital $3a_1$ should be the more effective nucleophile, especially in oxidative-addition reactions with sterically hindered electrophiles such as alkyl halides. There is no conflict with frontier orbital theory for this reason. Thus, in oxidative addition of methyl iodide, the $3a_1$ orbital

---

(39) Young, Y. Y.; Cheng, K. L. *J. Electron Spectrosc. Relat. Phenom.* **1976**, *9*, 317.

(40) Beach, D. B.; Bertoncello, R.; Granozzi, G.; Jolly, W. L. *Organometallics* **1985**, *4*, 311.

(41) Dignard, L. M. Ph.D. Thesis, University of Western Ontario, London, Canada, 1986.

(42) Bursten, B. E.; Fenske, R. F. *Inorg. Chem.* **1977**, *16*, 963. Fantucci, P.; Naldini, L.; Cariati, F.; Valenti, V.; Bussetto, C. *J. Organomet. Chem.* **1974**, *64*, 125.

(43) Clark, H. C.; Manzer, L. E.; Ward, J. E. H. *J. Organomet. Chem.* **1974**, *52*, 1165.

(44) Lappert, M. F.; Pedley, J. B.; Wilkins, B. T.; Stelzer, O.; Unger, E. *J. Chem. Soc., Dalton Trans.* **1975**, *43*, 1207. Magnusson, E. *Aust. J. Chem.* **1985**, *38*, 23; *J. Am. Chem. Soc.* **1984**, *106*, 1185. Eyermann, C. J.; Jolly, W. L. *J. Phys. Chem.* **1983**, *87*, 3080.

(45) Puddephatt, R. J.; Dignard, L. M.; Bancroft, G. M. *Inorg. Chim. Acta* **1985**, *96*, L91. Bancroft, G. M.; Dignard, L. M.; Puddephatt, R. J. *Inorg. Chem.* **1986**, *25*, 3675.

(46) Bush, R. C.; Angelici, R. J. *Inorg. Chem.* **1988**, *27*, 681.

of platinum would give S_N2 attack at the methyl group with displacement of iodide,[47] which subsequently coordinates to give octahedral $[PtIMe_3L_2]$. The reactivity depends in turn on the donor ability of L, and the series for reactivity to oxidative addition L_2 = TMED > R_3P > $(RO)_3P$ > COD, MeNC is fully consistent with the donor abilities of the ligands as deduced from the photoelectron spectra.[47]

A more difficult problem arises in determining the mechanism of cleavage of platinum–methyl bonds by electrophilic reagents. For example, the reaction of HCl with *cis*-$[PtMe_2L_2]$ gives methane and $[PtClMeL_2]$. Here the reaction could occur by oxidative addition of H^+ (as above, with an intermediate $[PtHMe_2L_2]^+$)[47] followed by reductive elimination of methane,[48] or the electrophile (H^+ in this example) could attack the Pt–Me σ MO directly[49] to give methane. The HOMO is believed to be the σ MO $4a_1$, and this makes the direct attack plausible, especially with the reagent H^+, which has low steric requirements. As discussed above, bulkier reagents would almost certainly attack the d-orbital $3a_1$, and this has been shown to occur with the electrophile Ph_3PAu^+, which is isolobal to H^+.[48] Since $3a_1$ and $4a_1$ are close in energy (and of the same symmetry so that mixing is predicted), it is possible that H^+ could attack either orbital. We note, however, that $4a_1$ is calculated to be very weakly bonding or even antibonding with respect to the Pt–Me groups and in some complexes it is localized to a greater extent on the ligands L (e.g. when L = C_2H_4). Attack of H^+ at the PtL bond would not lead to productive chemistry; the orbital $1a_1$, which is much more strongly Pt–Me bonding, is considerably lower in energy and is less likely to be involved in reactions with electrophiles. To summarize, the electronic structure of the complexes *cis*-$[PtMe_2L_2]$, in which d orbitals and σ MO's are close in energy, should allow electrophilic cleavage to occur by direct attack on the M–C bond or by oxidative addition–reductive elimination. Relaxation effects (steric or electronic in origin) are likely to have a considerable effect in determining which mechanism is preferred.

The complexes are also susceptible to nucleophilic attack, and $[PtMe_2(COD)]$ is often used as a precursor to other complexes $[PtMe_2L_2]$. The NBD ligand in $[PtMe_2(NBD)]$ is displaced even more readily.[50] These reactions are probably associative, using the empty 6p orbital on platinum as acceptor. Since the calculations indicate diffuse features for the lowest virtual orbitals, and the photoelectron spectra give no useful information either, the nature of these reactions will not be discussed further.

Conclusions

The UV photoelectron spectra of the dimethylplatinum(II) complexes can be assigned with the help of the resolved vibrational fine structures, substitution effects, and MS–Xα calculations, while the He II/He I area ratios are generally not useful. The first two molecular orbitals with low-IE values contain contributions from both Pt and ligand orbitals, and these are followed by the essentially nonbonding Pt 5d orbitals. The σ-donor ability falls in the order $P(NMe_2)_3$ > TMED > $PMePh_2$ ~ PMe_2Ph > PEt_3 > $AsMe_3$ ~ PMe_3 > $PMe(OEt)_2$ > $P(OEt)_3$ > $P(OMe)_3$ > COD, NBD, and the π-acceptor ability falls in the order $PMePh_2$ ~ PMe_2Ph ~ $P(OMe)_3$ ~ $P(OEt)_3$ ~ PMe(OEt) ~ $P(NMe_2)_3$ > $AsMe_3$ ~ PMe_3 ~ PEt_3 ~ COD ~ NBD > TMED. Both CNMe and CNPh have comparable σ-donor properties, and the latter has stronger π-donor and π-acceptor abilities. Some typical chemical reactions such as oxidative addition and electrophilic cleavage of a Pt–C bond leading to ligand replacement can be reasonably accounted for, on the basis of the established σ/π series and the ionization features.

Acknowledgment. We are grateful to the Natural Sciences and Engineering Research Council of Canada for financial support.

Supplementary Material Available: Figures S1–S3, showing He I spectra of *cis*-$[PtMe_2L_2]$, where L = PMe_3, PMe_2Ph, and $PMePh_2$, *cis*-$[PtMe_2L_2]$, where L = $P(OMe)_3$, $P(OEt)_3$, and $PMe(OEt)_2$, and *cis*-$[PtMe_2L_2]$, where L = MeNC and PhNC, and Tables S1–S3, listing MS–Xα results for upper valence orbitals of *cis*-$[PtMe_2(NH_3)_2]$, *cis*-$[PtMe_2(AsH_3)_2]$, and *cis*-$[PtMe_2(CNH)_2]$ (6 pages). Ordering information is given on any current masthead page.

---

(47) Kistner, C. R.; Drew, D. A.; Doyle, J. R.; Rausch, G. W. *Inorg. Chem.* **1967**, *6*, 2036. Usôn, R.; Forniês, J.; Espinet, P.; Gavin, J. *J. Organomet. Chem.* **1976**, *105*, C25. Jawad, J. K.; Puddephatt, R. J. *J. Organomet. Chem.* **1976**, *117*, 297. Jawad, J. K.; Puddephatt, R. J. *J. Chem. Soc., Dalton Trans.* **1977**, 1466. Monaghan, P. K.; Puddephatt, R. J. *Organometallics* **1985**, *4*, 1406. Kuyper, J. *Inorg. Chem.* **1978**, *17*, 77. Monaghan, P. K.; Puddephatt, R. J. *Organometallics* **1984**, *3*, 444. Ferguson, G.; Parvez, M.; Monaghan, P. K.; Puddephatt, R. J. *Organometallics* **1985**, *4*, 1669; *J. Chem. Soc., Chem. Commun.* **1983**, 267. Scott, J. D.; Puddephatt, R. J. *Inorg. Chim. Acta* **1984**, *89*, L27. Monaghan, P. K.; Puddephatt, R. J. *J. Chem. Soc., Dalton Trans.* **1988**, 595.

(48) Belluco, U.; Giustiniani, M.; Graziani, M. *J. Am. Chem. Soc.* **1967**, *89*, 6494. Jawad, J. K.; Puddephatt, R. J.; Stalteri, M. A. *Inorg. Chem.* **1982**, *21*, 332 and references therein. Arsenault, G. J.; Anderson, C. M.; Puddephatt, R. J. *Organometallics* **1988**, *7*, 2094.

(49) Romeo, R.; Minniti, D.; Lanza, S.; Uguagliati, P.; Belluco, U. *Inorg. Chem.* **1978**, *17*, 2813. Romeo, R.; Minniti, D.; Lanza, S. *J. Organomet. Chem.* **1979**, *165*, C36. Alibrandi, G.; Minniti, D.; Scolaro, L. M.; Romeo, R. *Inorg. Chem.* **1988**, *27*, 318.

(50) Appleton, T. G.; Hall, J. R.; Neale, D. W.; Williams, M. A. *J. Organomet. Chem.* **1984**, *276*, C73. Thorn, D. L.; Calabrese, J. C. *J. Organomet. Chem.* **1988**, *342*, 269.